Acta Crystallographica Section F
Structural Biology and Crystallization Communications
ISSN 1744-3091

Purification, crystallization and X-ray diffraction analysis of pavine *N*-methyltransferase from *Thalictrum flavum*

Ankur Jain,[a,b] Jörg Ziegler,[c] David K. Liscombe,[c] Peter J. Facchini,[c] Paul A. Tucker[a] and Santosh Panjikar[a]*

[a]EMBL Hamburg Outstation, c/o DESY, Notkestrasse 85, D-22603 Hamburg, Germany, [b]Indian Institute of Technology, Roorkee, India, and [c]Department of Biological Sciences, 2500 University Drive NW, University of Calgary, Calgary, Alberta T2N 1N4, Canada

Correspondence e-mail: panjikar@embl-hamburg.de

Received 13 August 2008
Accepted 12 October 2008

A cDNA from the plant *Thalictrum flavum* encoding pavine *N*-methyltransferase, an enzyme belonging to a novel class of *S*-adenosylmethionine-dependent *N*-methyltransferases specific for benzylisoquinoline alkaloids, has been heterologously expressed in *Escherichia coli*. The enzyme was purified using affinity and gel-filtration chromatography and was crystallized in space group $P2_1$. The structure was solved at 2.0 Å resolution using a xenon derivative and the single isomorphous replacement with anomalous scattering method.

1. Introduction

S-Adenosyl-L-methionine-dependent *N*-methyltransferases (NMTs) occur in several plant biosynthetic pathways and are especially common in secondary metabolism. Many NMTs involved in plant secondary metabolism catalyze key reactions in alkaloid biosynthesis (Ziegler & Facchini, 2008). For example, putrescine *N*-methyltransferase (PMT) catalyzes the first committed step in the formation of nicotine (Hibi *et al.*, 1994) and tropane alkaloids such as hyoscyamine and scopolamine (Teuber *et al.*, 2007). Purine alkaloid biosynthesis involves several NMTs with different regiospecificities and substrate specificities, leading to monomethylated, dimethylated and trimethylated purine alkaloids including caffeine and theobromine (Uefuji *et al.*, 2003). An NMT also participates in the biosynthesis of the monoterpenoid indole alkaloid vindoline, which is a precursor of the anti-cancer drug vinblastine (Dethier & De Luca, 1993). Several NMTs must also play a role in the formation of the structurally diverse benzylisoquinoline alkaloids based on the occurrence of a multitude of *N*-methylated and *N*,*N*-dimethylated compounds (Shulgin & Perry, 2002). Cognate cDNAs encoding two NMTs involved in benzylisoquinoline alkaloid metabolism have been isolated. Coclaurine *N*-methyltransferase (CNMT) catalyzes the *N*-methylation of simple benzylisoquinoline alkaloids in the core pathway (Choi *et al.*, 2002), whereas tetrahydroprotoberberine *N*-methyltransferase (TNMT) exhibits specificity for certain intermediates in the protoberberine branch pathway (Liscombe & Facchini, 2007). Phylogenetic analysis has shown that plant NMTs belong to different clades that are generally separated according to the metabolic pathways in which they operate. Thus, PMTs form a clade together with spermidine synthases and are well separated from the NMTs involved in caffeine biosynthesis, which belong to the SABATH (salicylic acid carboxylmethyltransferase, benzoic acid carboxylmethyltransferase, theobromine synthase) family of methyltransferases. NMTs involved in benzylisoquinoline alkaloid biosynthesis form a separate clade that is more closely related to cyclopropane fatty-acid synthases (Liscombe & Facchini, 2007). Recently, four cDNAs encoding novel NMTs were obtained from expressed sequence-tag databases for several benzylisoquinoline alkaloid-producing plant-cell cultures (D. Liscombe, J. Ziegler & P. Facchini, unpublished results). Two of these NMTs showed overlapping substrate specificities, whereas the others showed unique substrate preferences. Among them was an NMT from *Thalictrum flavum* which catalyzes the *N*-methylation of pavine

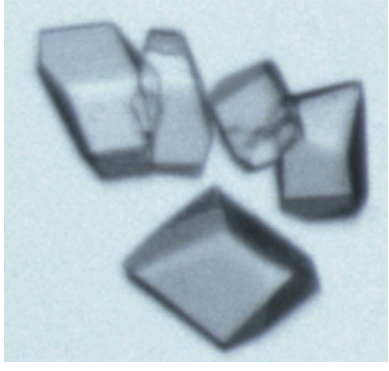

to *N*-methylpavine (PavNMT). The details of this work will be published elsewhere.

Based on the multitude of possible substrates of the NMTs involved in benzylisoquinoline alkaloid metabolism and the likely occurrence of additional NMTs with distinct substrate specificities, we are interested in the molecular mechanism responsible for substrate discrimination. Moreover, the catalytic mechanism of these NMTs has not yet been investigated. Structural information based on crystallographic data has only been obtained for NMTs involved in caffeine biosynthesis (McCarthy & McCarthy, 2007). A three-dimensional protein model of PMT has also been created based on its sufficient similarity to spermidine synthase (Teuber *et al.*, 2007). No structural information is available for CNMT or for TNMT and homology-based approaches are hampered by their low similarity compared with structurally characterized proteins. Towards the goal of determining the X-ray structure of PavNMT, His-tagged PavNMT from *T. flavum* was produced in *Escherichia coli*, purified and crystallized.

2. Experimental methods

2.1. Cloning of the PavNMT cDNA from *T. flavum*

A full-length EST encoding PavNMT was identified from a cDNA library prepared from RNA isolated from *T. flavum* cell cultures using the *tBLASTn* algorithm (Altschul *et al.*, 1990) in the *FIESTA* software platform (National Research Council Plant Biotechnology Institute, Saskatoon, Canada). It was selected for further characterization based on its substantial similarity to known benzylisoquinoline alkaloid NMTs (Choi *et al.*, 2002; Liscombe & Facchini, 2007). The PavNMT open reading frame (residues 1–386) was amplified with *Pfu* polymerase (Fermentas, Burlington, Canada) using sense primers specific for the 5′-end and an antisense primer corresponding to the T7 annealing site in pBluescript SK−. A *Kpn*I restriction site was included at the 5′-end of the sense primer. Amplicons were cloned into pRSETC (Invitrogen, Carlsbad, California, USA) after digestion with *Pvu*II and *Kpn*I.

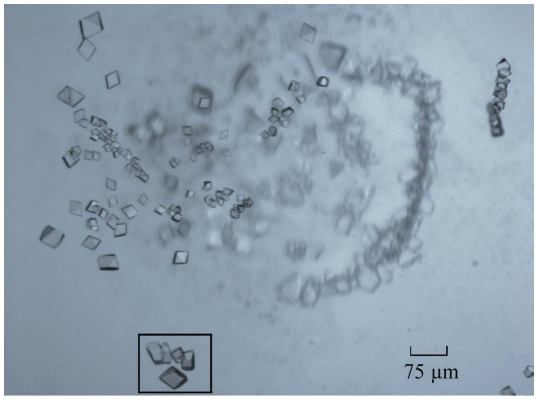

(*a*)

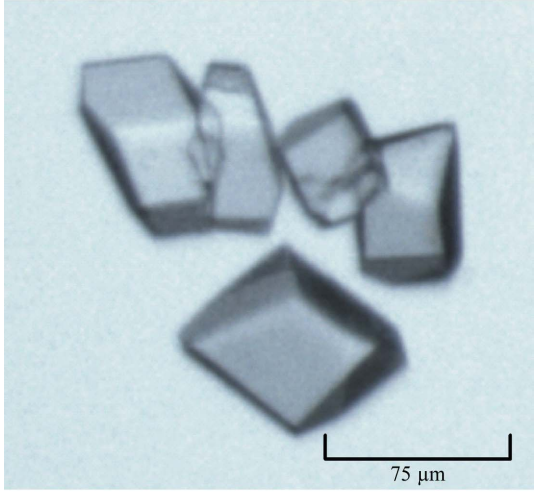

(*b*)

Figure 1
Crystals of *T. flavum* PavNMT. (*a*) Primitive monoclinic crystals obtained by the hanging-drop method. (*b*) Enlarged picture of crystals from the marked area in Fig. 1(*a*).

2.2. Production and purification of recombinant PavNMT from *T. flavum*

BL21(DE3)pLysS cells transformed with the pRSETC-PavNMT construct were grown overnight in 4 ml Luria–Bertani (LB) medium supplemented with 50 µg ml^{-1} ampicillin and 34 µg ml^{-1} chloramphenicol at 310 K. The overnight cultures were used to inoculate 4 × 1 l liquid cultures and the cells were grown at 310 K to a cell density of 0.5 OD_{600}. Recombinant protein production was induced with 1 m*M* isopropyl β-D-1-thiogalactopyranoside. After incubation at room temperature to a cell density of 1.4 OD_{600}, cells were harvested and sonicated in extraction buffer [20 m*M* Tris–HCl pH 7.5, 100 m*M* KCl, 10%(*v*/*v*) glycerol, 10 µg ml^{-1} lysozyme]. After removal of the cell debris by centrifugation, the supernatant was loaded onto a Talon cobalt-affinity column (Clontech, Mountain View, California, USA), which was subsequently washed with extraction buffer without lysozyme. The recombinant protein was eluted by a stepwise increase in the imidazole concentration from 10 to 100 m*M*. The fractions with the highest PavNMT protein content (*i.e.* the fractions eluted with 50–100 m*M* imidazole) were concentrated using 30 kDa nominal molecular-weight limit Amicon Ultra-15 ultrafiltration devices (Millipore, Billerica, Massachusetts, USA) and loaded onto a Superose 12 HR 10/30 gel-filtration column (Amersham, Piscataway, New Jersey, USA) equilibrated in extraction buffer. Elution of the protein was performed using extraction buffer at a flow rate of 1 ml min^{-1} and was monitored by absorption at 280 nm. Fractions containing PavNMT were concentrated as described above and the buffer was exchanged to 20 m*M* Tris–HCl pH 7.4, 100 m*M* KCl and 1%(*v*/*v*) glycerol using PD10 columns (Amersham). After an additional protein-concentration step using ultrafiltration as described above, the protein concentration was determined with a spectrophotometer at 280 nm using a molar extinction coefficient of 69 400 cm M^{-1} as determined by the amino-acid sequence of the His-tagged recombinant protein.

2.3. Crystallization

Purified recombinant PavNMT (concentration 11.3 mg ml^{-1}) in Tris buffer pH 7.4 containing 10 m*M* KCl and 1%(*v*/*v*) glycerol was initially screened for crystallization conditions using the high-throughput crystallization facility operated by EMBL Hamburg, Germany (Mueller-Dieckmann, 2006). Initial crystallization screens were performed using the sitting-drop vapour-diffusion method with Crystal Screen and Crystal Screen Cryo (Hampton Research, Aliso Viejo, California, USA) based on 288 different conditions. Each drop consisted of 0.2 µl protein solution and 0.2 µl precipitant solution. Microcrystals were obtained in 0.2 *M* ammonium acetate, 0.1 *M* bis-tris pH 5.5 and 30%(*w*/*v*) PEG 4000 after 24 h at 289 K.

PavNMT crystals were manually reproduced at 289 K using the hanging-drop vapour-diffusion method and the crystallization con-

dition was optimized. The volume of the drop was 2 µl and consisted of a mixture of 1 µl protein solution and 1 µl precipitant solution. The drop was equilibrated over a reservoir filled with 1 ml 0.2 *M* ammonium acetate, 0.1 *M* bis-tris pH 5.5 and 19.5%(*w*/*v*) PEG 4000. Bipyramid-shaped crystals grew to 75 µm in their longest dimension in 2 d (Fig. 1).

2.4. Xenon derivatization

A crystal was transferred into cryoprotectant [20%(*v*/*v*) glycerol, 6.5%(*w*/*v*) PEG 4000] and picked up in a cryo-loop, which was then transferred to a pressure cell (Hampton Research) and pressurized under a 3.6 MPa xenon atmosphere for 1 min. The pressure was released over 30 s and the crystal was immediately flash-cooled in liquid nitrogen (Soltis *et al.*, 1997; Panjikar & Tucker, 2002).

2.5. Diffraction data collection and processing

Prior to data collection, a single native crystal of PavNMT was treated with the cryoprotectant for 30 s and flash-cooled to 100 K in liquid nitrogen. It was exposed at an X-ray wavelength of 1.0000 Å and 200° of native data were collected with 1° oscillation per image and an exposure time of 0.12 s at a crystal-to-detector distance of 283.1 mm. The crystal diffracted to beyond 2.0 Å resolution.

For phasing purposes, a single native crystal of similar size was derivatized with xenon. X-ray data from the crystal were collected with 1° oscillation per image and an exposure time of 0.29 s at a crystal-to-detector distance of 152.13 mm and an X-ray wavelength of 1.7 Å. A total of 360° of data were collected to 2.2 Å resolution. Both diffraction data sets were collected on ESRF beamline ID29 (Grenoble, France) using an ADSC Q4 (Area Detector Systems Cooperation) CCD detector. The EMBL/ESRF/BM14 robotic sample changer (SC3) at the beamline allowed rapid screening of various crystals (Cipriani *et al.*, 2006). In addition, the MD2M mini-diffractometer installed at the beamline permitted precise centring of the small crystals.

The data sets were indexed and integrated using *XDS* (Kabsch, 1993). The relevant data-collection and processing parameters are given in Table 1. Intensities were converted to structure-factor amplitudes using the program *TRUNCATE* (French & Wilson, 1978; Collaborative Computational Project, Number 4, 1994). The optical resolution was calculated using the program *SFCHECK* (Vaguine *et al.*, 1999; Collaborative Computational Project, Number 4, 1994).

3. Results and discussion

The purified recombinant protein contained an additional vector-derived 11-amino-acid sequence MRGSHHHHHHG between the N-terminal Met and the second amino acid Gly of the native PavNMT sequence, resulting in a protein consisting of 397 amino acids with a calculated molecular weight of 46 400 Da. PavNMT was purified with a yield of about 1–2 mg per litre of bacterial culture and with a purity of approximately 96% as judged by SDS–PAGE. Based on the gel-filtration elution profile, the apparent molecular weight of the protein in solution was approximately 85 000 Da, which is consistent with the molecular weight of a homodimer.

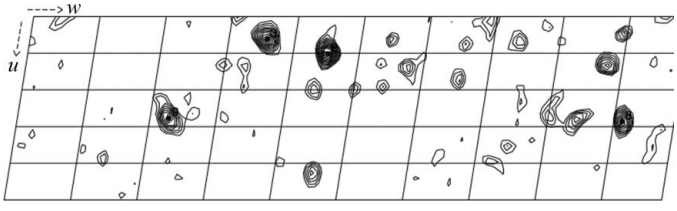

Figure 2
Harker section of the anomalous difference Patterson map for the xenon derivative of the PavNMT crystal. The stronger peaks indicate the xenon sites, whereas the weaker peaks show either low-occupancy xenon sites or sulfur positions.

Table 1
Data-collection and processing statistics.

Values in parentheses are for the highest resolution bin.

	Native	Xenon derivative
No. of crystals	1	1
Wavelength (Å)	1.00	1.70
Crystal-to-detector distance (mm)	283.1	152.13
Total rotation range (°)	200	360
Resolution range (Å)	99.0–2.00 (2.05–2.00)	99.0–2.20 (2.15–2.20)
Space group	$P2_1$	$P2_1$
Unit-cell parameters (Å, °)	a = 54.11, b = 71.93, c = 96.64, β = 98.8	a = 54.19, b = 72.23, c = 96.67, β = 99.1
Mosaicity (°)	0.14	0.21
Total No. of reflections	205275	270403
Unique reflections	49502	71355
Redundancy	4.1	3.8
$\langle I/\sigma(I)\rangle$	17.34 (3.8)	15.34 (2.6)
Completeness (%)	99.8 (99.4)	96.8 (93.4)
$R_{\rm merge}$† (%)	6.0 (38.5)	6.3 (50.6)
$R_{\rm r.i.m.}$‡ (%)	6.9 (42.7)	7.0 (59.7)
Overall B factor from Wilson plot (Å^2)	26.0	39.3
Optical resolution (Å)	1.57	1.73

† $R_{\rm merge} = \sum_{hkl}\sum_i |I_i(hkl) - \langle I(hkl)\rangle| / \sum_{hkl}\sum_i I_i(hkl)$ (Stout & Jensen, 1968), where $I_i(hkl)$ is the intensity of the ith measurement of reflection hkl and $\langle I(hkl)\rangle$ is the average intensity of a reflection. ‡ $R_{\rm r.i.m.}$ is the redundancy-independent merging R factor (Weiss & Hilgenfeld, 1997), which is identical to the $R_{\rm meas}$ of Diederichs & Karplus (1997*a*,*b*). $R_{\rm r.i.m} = \sum_{hkl}[N/(N-1)]^{1/2}\sum_i |I_i(hkl) - \langle I(hkl)\rangle| / \sum_{hkl}\sum_i I_i(hkl)$, with N being the number of times a given reflection has been observed.

Complete X-ray diffraction data sets were collected to 2.00 and 2.20 Å resolution for the native and xenon-derivative crystals, respectively (Table 1). The crystals belonged to the primitive monoclinic space group $P2_1$. Based on the protein molecular weight of 46 400 Da, the most likely number of molecules in the asymmetric unit was two, corresponding to a Matthews parameter $V_{\rm M}$ of 2.08 Å^3 Da^{-1} and a solvent content of 41% (Matthews, 1968). A self-rotation function displayed only one noncrystallographic twofold axis between the crystallographic x and y axes, confirming the presence of two molecules in the asymmetric unit.

Attempts to solve the three-dimensional structure by molecular replacement using the crystal structure of *Mycobacterium tuberculosis* mycolic acid cyclopropane synthase (MtPcaA; PDB code 1l1e; Huang *et al.*, 2002) as a search model were unsuccessful. The failure of the molecular replacement is probably a result of the low (23%) degree of sequence identity between the search model and PavNMT. Therefore, native crystals were derivatized under a xenon atmosphere. The presence of xenon sites was confirmed from a Harker section of an anomalous difference Patterson map of the xenon derivative (Fig. 2). The derivative data set had an overall isomorphous R factor of 22% with the native. The structure was solved *in situ* using the single isomorphous replacement with anomalous scattering (SIRAS) protocol of *Auto-Rickshaw* (Panjikar *et al.*, 2005). The details of the structure determination and analysis will be published elsewhere. Comparison of the structure of PavNMT with those of other methyltransferase structures will provide insight into the molecular mechanism of this important enzyme.

We would like to thank the DAAD academic exchange programme for providing financial support to AJ during his stay at the EMBL Hamburg Outstation, Germany (grant No. GR 6208-A0807128) and

the ESRF (Grenoble, France) for the allocation and provision of beamtime. DKL is the recipient of a Natural Sciences and Engineering Research Council (NSERC) of Canada postgraduate scholarship. PJF is the Canada Research Chair of Plant Metabolic Processes Biotechnology and thanks NSERC for funding in support of this work.

References

Altschul, S. F., Gish, W., Miller, W., Myers, E. W. & Lipman, D. J. (1990). *J. Mol. Biol.* **215**, 403–410.
Choi, K. B., Morishige, T., Shitan, N., Yazaki, K. & Sato, F. (2002). *J. Biol. Chem.* **277**, 830–835.
Cipriani, F. *et al.* (2006). *Acta Cryst.* D**62**, 1251–1259.
Collaborative Computational Project, Number 4 (1994). *Acta Cryst.* D**50**, 760–763.
Dethier, M. & De Luca, V. (1993). *Phytochemistry*, **32**, 673–678.
Diederichs, K. & Karplus, P. A. (1997*a*). *Nature Struct. Biol.* **4**, 269–275.
Diederichs, K. & Karplus, P. A. (1997*b*). *Nature Struct. Biol.* **4**, 592.
French, S. & Wilson, K. (1978). *Acta Cryst.* A**34**, 517–525.
Hibi, N., Higashiguchi, S., Hashimoto, T. & Yamada, Y. (1994). *Plant Cell*, **6**, 723–735.
Huang, C. C., Smith, C. V., Glickman, M. S., Jacobs, W. R. Jr & Sacchettini, J. C. (2002). *J. Biol. Chem.* **277**, 11559–11569.
Kabsch, W. (1993). *J. Appl. Cryst.* **26**, 795–800.
Liscombe, D. K. & Facchini, P. J. (2007). *J. Biol. Chem.* **282**, 14741–14751.
Matthews, B. W. (1968). *J. Mol. Biol.* **33**, 491–497.
McCarthy, A. A. & McCarthy, J. G. (2007). *Plant Physiol.* **144**, 879–889.
Mueller-Dieckmann, J. (2006). *Acta Cryst.* D**62**, 1446–1452.
Panjikar, S., Parthasarathy, V., Lamzin, V. S., Weiss, M. S. & Tucker, P. A. (2005). *Acta Cryst.* D**61**, 449–457.
Panjikar, S. & Tucker, P. A. (2002). *J. Appl. Cryst.* **35**, 117–119.
Shulgin, A. T. & Perry, W. E. (2002). *The Simple Plant Isoquinolines*. Berkeley, USA: Transform Press.
Soltis, S. M., Stowell, M. H. B., Wiener, M. C., Phillips, G. N. & Rees, D. C. (1997). *J. Appl. Cryst.* **30**, 190–194.
Stout, G. H. & Jensen, L. H. (1968). *X-ray Structure Determination. A Practical Guide*, p. 402. London: Macmillan.
Teuber, M., Azemi, M. E., Namjoyan, F., Meier, A. C., Wodak, A., Brandt, W. & Dräger, B. (2007). *Plant Mol. Biol.* **63**, 787–801.
Uefuji, H., Ogita, S., Yamaguchi, Y., Koizumi, N. & Sano, H. (2003). *Plant Physiol.* **132**, 372–380.
Vaguine, A. A., Richelle, J. & Wodak, S. J. (1999). *Acta Cryst.* D**55**, 191–205.
Weiss, M. S. & Hilgenfeld, R. (1997). *J. Appl. Cryst.* **30**, 203–205.
Ziegler, J. & Facchini, P. J. (2008). *Annu. Rev. Plant Biol.* **59**, 735–769.